



## Purinergic signaling mediates oxidative stress in UVA-exposed THP-1 cells



Ayumi Kawano<sup>a</sup>, Akimitsu Hayakawa<sup>a</sup>, Shuji Kojima<sup>b</sup>, Mitsutoshi Tsukimoto<sup>b</sup>, Hikaru Sakamoto<sup>a,\*</sup>

<sup>a</sup> Radioisotope Research Laboratory, School of Pharmacy, Kitasato University, 5-9-1 Shirokane, Minato-ku, Tokyo, Japan

<sup>b</sup> Department of Radiation Biosciences, Faculty of Pharmaceutical Sciences, Tokyo University of Science, 2641 Yamazaki, Noda-shi, Chiba, Japan

### ARTICLE INFO

#### Article history:

Received 26 January 2015

Accepted 26 January 2015

Available online 7 February 2015

#### Keywords:

Ultraviolet A

ATP

P2X7 receptor

Reactive oxygen species

Cell death

### ABSTRACT

Ultraviolet A (UVA) radiation, the major UV component of solar radiation, can penetrate easily to the dermis, where it causes significant damage to cellular components by inducing formation of reactive oxygen species (ROS). On the other hand, extracellular ATP is released in response to various stimuli, and activates purinergic P2X7 receptor, triggering ROS production and cell death. Here, we examined the hypothesis that ATP release followed by activation of P2X7 receptor plays a role in UVA-induced oxidative cell damage, using human acute monocytic leukemia cell line THP-1. Indeed, UVA irradiation of THP-1 cells induced ATP release and activation of P2X7 receptor. Irradiated cells showed a rapid increase of both p67<sup>phox</sup> in membrane fraction and intracellular ROS. Pretreatment with ecto-nucleotidase or P2X7 receptor antagonist blocked the UVA-initiated membrane translocation of p67<sup>phox</sup> and ROS production. Furthermore, pretreatment with antioxidant or P2X7 receptor antagonist efficiently protected UVA-irradiated cells from caspase-dependent cell death. These findings show that autocrine signaling through release of ATP and activation of P2X7 receptor is required for UVA-induced stimulation of oxidative stress in monocytes.

© 2015 The Authors. Published by Elsevier Ireland Ltd. This is an open access article under the CC BY-NC-ND license (<http://creativecommons.org/licenses/by-nc-nd/4.0/>).

### 1. Introduction

Ultraviolet (UV) irradiation is divided into three wavelength ranges: UVA, UVB, and UVC. UVA covers the wavelength range 320–400 nm, and is the major component of UV exposure encountered in daily life [1]. Unlike UVB that cannot penetrate much deeper than the epidermis of the skin, it is estimated that about 50% of incident UVA penetrates Caucasian skin all the way to the dermis, and is capable of irradiating blood leukocytes passing through

skin capillaries [2,3,41]. Polderman et al. [3] reported that UVA caused cell death of peripheral blood mononuclear cells, and monocytes seemed to be the most sensitive to UVA among white cells. However, it is still unclear how monocytes are impaired by UVA irradiation.

UVA-induced damage occurs mainly via oxidative stress at the cellular level, and UVA is considered as the most important oxidizing agent in human skin [42]. Exposure of skin to UVA results in the generation of large amounts of intracellular reactive oxygen species (ROS), which directly or indirectly affect various cell signaling pathways, as well as augmenting various UV-induced cutaneous reactions including inflammation, photosensitivity and carcinogenesis [4,5]. Singlet oxygen ( ${}^1\text{O}_2$ ), the major ROS, is formed in cells by energy transfer to molecular oxygen from the triplet excited state of endogenous

\* Corresponding author at: Radioisotope Research Laboratory, School of Pharmacy, Kitasato University, 5-9-1 Shirokane, Minato-ku, Tokyo 108-8641, Japan. Tel.: +81 03 3444 4944; fax: +81 03 3444 4944.

E-mail address: [sakamotohi@pharm.kitasato-u.ac.jp](mailto:sakamotohi@pharm.kitasato-u.ac.jp) (H. Sakamoto).

chromophores. The endogenous chromophores and their locations in mammalian cells have not been identified, but many chromophores such as porphyrins, NAD (P) H, flavins, and other enzyme cofactors have been considered as photobiologically active [6]. It is well known that  $^1\text{O}_2$  contributes to UVA-induced responses [7,43]. However, other ROS are involved in UVA-induced responses, because the lifetime of  $^1\text{O}_2$  in cells is very short [8,9], and ROS are detected long after the end of UVA exposure [10]. Among UVA-induced ROS, superoxide ( $\text{O}_2^-$ ) and hydrogen peroxide can destroy normal cell structure and function, resulting in tissue injury [11]. Godar [43] reported that UVA radiation triggers two different apoptotic pathways, mediated by  $^1\text{O}_2$  or  $\text{O}_2^-$ . Thus, ROS produced subsequent to  $^1\text{O}_2$  appear to play a key role in UVA-induced cellular responses.

The purinergic P2X7 receptor belongs to the family of purinoreceptors for ATP, and is expressed in various immune cells, including monocytes [12]. Upon ATP stimulation, P2X7 receptor opens a cation channel, which permits  $\text{K}^+$  influx, and gradually forms a larger pore on the membrane [13]. Since activation of P2X7 receptor results in membrane blebbing [14], ROS production via NADPH oxidase activation [15], and apoptotic and/or necrotic cell death [16], P2X7 receptor appears to have an important role in regulating inflammation. Cells injured at sites of inflammation can passively release ATP in amounts sufficient to activate P2X7 receptor. It was recently reported that agonists of different pattern recognition receptors trigger release of endogenous ATP and stimulate P2X7 receptor in human monocytes [17]. However, it is unknown whether UVA irradiation of monocytes evokes ATP release and subsequent activation of P2X7 receptor.

The objective of the present study was to examine whether autocrine signaling through ATP-P2X7 receptor is involved in UVA-induced ROS production and caspase-dependent death of human monocytes. Our results suggest that ATP released from cells activates P2X7 receptor, and this leads to formation of ROS. These findings indicated that autocrine ATP signaling contributes to UVA-induced cellular injury of monocytes.

## 2. Materials and methods

### 2.1. Reagents and antibodies

L-Ascorbic acid and probenecid were purchased from Wako Pure Chemical Industries (Osaka, Japan). MnTMyP was purchased from Merck (Darmstadt, Germany). Caspase-3 antibody, caspase-9 antibody, goat horseradish peroxidase (HRP)-conjugated anti-rabbit IgG antibody and goat HRP-conjugated anti-mouse IgG antibody were purchased from Cell Signaling Technology, Inc. (Beverly, MA). Purified mouse anti-p67 and purified mouse anti-flotillin-1 were purchased from BD Biosciences (San Jose, CA). Mouse anti- $\beta$ -actin antibody was purchased from Santa Cruz Biotechnology, Inc. (Santa Cruz, CA). Unless otherwise stated, all other reagents were obtained from Sigma Aldrich (St. Louis, MO). All chemicals used were of the highest purity available.

### 2.2. Cell culture and irradiation

THP-1 human acute monocytic leukemia cells (American Type Culture Collection) were grown in RPMI 1640 medium (Wako), supplemented with 10% fetal bovine serum (HyClone Laboratories, South Logan, UT), penicillin (100 units/mL) and streptomycin (100  $\mu\text{g}/\text{mL}$ ) (Sigma-Aldrich) in a humidified atmosphere of 5%  $\text{CO}_2$  in air at 37 °C.

The medium was removed, and cells were washed twice with phosphate-buffered saline (PBS) before UVA irradiation. The medium was replaced with RPMI Medium 1640 (without Phenol Red) (Life Technologies, Carlsbad, CA), and then UVA irradiation was performed. The UVA irradiation source was a black light (UVA) lamp (Sankyo Denki, Tokyo, Japan) with peak energy emission at 360 nm. The emitted dose was measured with a radiometer (UVX-36; UVP, Inc., San Gabriel, CA). No UVB component was detected with a UVX-31 sensor (UVP, Inc.). The irradiance at the sample level was about 2.5 mW/cm<sup>2</sup>. The cooling control device was used to prevent excessive temperature rise by the generation of heat (Preset temperature is 21 °C).

### 2.3. Detection of ROS level

ROS were assayed with ROS indicator 6-carboxy-2',7'-dichlorodihydrofluorescein diacetate (carboxy-H<sub>2</sub>DCFDA) (Molecular Probes, Eugene, OR). Cells were loaded with 10  $\mu\text{M}$  carboxy-H<sub>2</sub>DCFDA for 30 min at 37 °C and washed twice with PBS. After UVA irradiation, fluorescence was detected using a dual-scanning microplate spectrofluorometer (SpectraMax M5, Molecular Devices, Orleans, CA) with 485 nm excitation and 538 nm emission, or visualized with a fluorescence microscope (Olympus, Tokyo, Japan).

### 2.4. Immunoblotting

Aliquots of samples (10  $\mu\text{g}$  per lane) were separated by means of 10% SDS-PAGE and transferred onto a PVDF membrane. Blots were incubated for 2 h at room temperature in Tris-buffered saline containing 0.1% Tween 20 (TBS-T) (10 mM Tris-HCl, 100 mM NaCl, 0.1% Tween 20, pH 7.5) with 1% BSA and incubated at 4 °C overnight with purified mouse anti-p67 (1:1000), caspase-3 antibody (1:1000), or caspase-9 antibody (1:1000). Purified mouse anti-flotillin-1 (1:1000) and anti- $\beta$ -actin antibody (1:1000) were used to confirm equal loading. Blots were washed with TBS-T, incubated with goat HRP-conjugated anti-rabbit IgG antibody (1:20,000) or goat HRP-conjugated anti-mouse IgG antibody (1:20,000) for 30 min at room temperature, and washed again with TBS-T. Specific proteins were visualized using ECL Western blotting detection reagents (GE Healthcare, Buckinghamshire, UK).

### 2.5. Cell fractionation

Cellular membrane fraction was prepared with the Mem-PER™ Eukaryotic Membrane Protein Extraction Reagent kit (Pierce Chemical, Rockford, IL) according to the manufacturer's instructions. Cells were washed with PBS twice and the cell pellet was lysed at room temperature

using cell lysis buffer (Reagent A). The membrane proteins were solubilized on ice with membrane solubilization buffer (Reagent C), which was diluted 2:1 with detergent dilution buffer (Reagent B). Reagent A and Reagents B/C include protease inhibitor cocktail (Sigma-Aldrich). The solubilized protein mixture was centrifuged at  $10,000 \times g$  for 3 min at  $4^\circ\text{C}$  to remove cellular debris. The clarified supernatant was heated at  $37^\circ\text{C}$  for 20 min, and then centrifuged at  $10,000 \times g$  for 2 min to separate the membrane and hydrophilic protein fractions. The membrane proteins were dissolved in  $2 \times$  sample buffer (25% glycerin, 1% SDS, 62.5 mM Tris-Cl, 10 mM DTT) after removal of detergent with an SDS-PAGE Sample Prep Kit (Pierce Chemical), and the solution was boiled for 10 min. Samples were analyzed by Western blotting as described above.

#### 2.6. Measurement of extracellular ATP

Extracellular ATP concentration was measured by using ENLITEN® rLuciferase/Luciferin Reagent (Promega, Madison, WI). After irradiation, culture supernatant was collected at the indicated time points. Each sample was centrifuged at  $600 \times g$  for 1 min and 10  $\mu\text{L}$  of the supernatant was used for ATP determination. Luciferin-luciferase reagent (100  $\mu\text{L}$ ) was added to the supernatant, and the chemiluminescence was measured with a SpectraMax M5. The ATP concentration in each sample was determined by comparing the luminescence of samples with those of standards in the range of  $10^{-6}$ – $10^{-9}$  M.

#### 2.7. Quantification of lactate dehydrogenase (LDH) release

Release of LDH into cell culture supernatant was quantified with a Cytotoxicity Detection Kit (Roche Applied Science, Basel, Switzerland), according to the manufacturer's instructions. After UVA irradiation, cells were incubated for 30 min. At the end of incubation, supernatants were collected and the LDH content was measured. LDH release is expressed as a percentage of the total content determined by lysing an equal amount of cells with lysis buffer.

#### 2.8. Analysis of pore formation

After UVA irradiation, ethidium bromide (EtBr) was added to the culture medium and incubation was continued for 5 min. The fluorescence was detected with a SpectraMax M5 set at 485 nm excitation and 612 nm emission, or visualized with a fluorescence microscope (Olympus).

#### 2.9. siRNA transfection

Transient transfection with siRNA against human P2RX7 (#1: Cat. SI000039508 and #2: SI00039515) (Qiagen, Milan, Italy) was performed according to the manufacturer's instructions. Negative control siRNA (Cat. 1022076) (Qiagen) was used as a control. A suspension of THP-1 cells ( $1.0 \times 10^6$  cells/mL) was diluted with an equal volume of

serum-free RPMI containing HiPerFect transfection reagent (Qiagen) and siRNA (100 nM). After 6 h, the cell suspension was further diluted 1:2 with fresh complete culture medium. Transfected cells were maintained in culture for up to 48 h before being used for the analysis.

#### 2.10. Analysis of cell viability

Cellular viability was determined by means of 3-[4,5-dimethylthiazol-2-yl]-2,5-diphenyltetrazolium bromide (MTT) assay. The MTT solution was added to a final concentration of 0.05%. After incubation for 4 h at  $37^\circ\text{C}$  in a humidified air atmosphere containing 5% CO<sub>2</sub>, stop solution (0.04 M HCl/isopropanol) was added and the mixture was incubated for 24 h. The absorption at 595 nm was measured with an iMark microplate reader (Bio-Rad, Hercules, CA).

#### 2.11. Morphological detection of apoptosis

Morphological changes characteristic of apoptosis were assessed by fluorescence microscopy after staining with the DNA-binding fluorochrome Hoechst 33342 (Dojindo). After UVA irradiation, cells were incubated for 3 h, then washed twice with PBS, and stained with Hoechst 33342 for 10 min at room temperature. The cells were then examined with a fluorescence microscope (Olympus) to evaluate nuclei fragmentation and chromatin condensation. The number of apoptotic nuclei in the microscopic field was counted.

#### 2.12. Statistics

Results are expressed as mean  $\pm$  SD. The statistical significance of differences between two groups was calculated by using the unpaired Student's *t*-test, and multiple groups were compared using ANOVA followed by pairwise comparisons with Bonferroni's *post hoc* analysis. Calculation was done with GraphPad prism 6.0 (GraphPad Software, San Diego, CA). The criterion of significance was set as  $P < 0.05$ .

### 3. Results

#### 3.1. UVA induces sustained ROS production in THP-1 cells

As shown in Fig. 1A, a significant and dose-dependent increase of DCF fluorescence occurred in response to UVA exposure. Previous studies have indicated that exposure of epidermal keratinocytes to  $10\text{J/cm}^2$  UVA or more causes molecular and cellular damage related to photoaging and photocarcinogenesis [18,19], and approximately half of total radiation dosage of UVA is absorbed by the epidermis [3]. Based on these viewpoints, a dose of  $5\text{J/cm}^2$  UVA was selected for further experiments. The fluorescence intensity peaked at 5 min, and remained elevated for 60 min. To examine whether the increase in DCF fluorescence reflected elevation of intracellular ROS, cells were pretreated with antioxidant, L-ascorbic acid (L-aa), or a membrane-permeable SOD mimetic, MnTMPyP. L-aa or

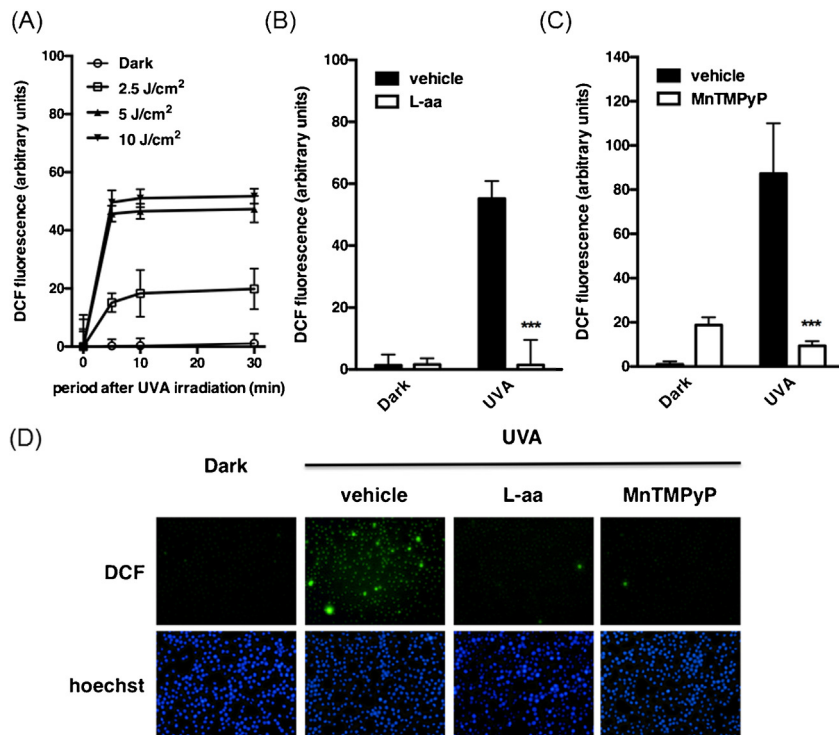


**Fig. 1.** ROS production in response to UVA in THP-1 cells. (A) Cells loaded with carboxy-H<sub>2</sub>DCFDA were irradiated with various doses of UVA. ROS generation was measured with DCF at the indicated time points after UVA irradiation. The fluorescence was analyzed with a fluorometer. Each value represents the mean  $\pm$  SD ( $n=4$ ). Next, cells loaded with carboxy-H<sub>2</sub>DCFDA were pre-incubated with vehicle alone or (B) L-ascorbic acid (1 mM) or (C) MnTMyP (5  $\mu$ M) for 30 min, then irradiated with 5 J/cm<sup>2</sup>, and incubated for 5 min. The fluorescence was analyzed with a fluorometer. Each value represents the mean  $\pm$  SD ( $n=4$ ). Significant differences between the irradiated control groups and the indicated groups are indicated by \*\*\* ( $P<0.001$ ). (D) DCF fluorescence was detected by fluorescence microscopy; similar results were obtained in three independent experiments, and typical images are presented.

MnTMyP significantly reduced the UVA-induced ROS production (Fig. 1B and C). Fluorescence microscopy images also showed a marked increase of DCF fluorescence in UVA-irradiated cells, and confirmed that pretreatment with L-aa or MnTMyP dramatically decreased the UVA-mediated ROS production (Fig. 1D). These results indicate that UVA irradiation can induce sustained ROS production in THP-1 cells.

### 3.2. NADPH oxidase is a major source of UVA-induced ROS production

Exposure to UVA has been reported to activate NADPH oxidase and to trigger rapid cellular oxidation in keratinocytes [10]. Activation of NADPH oxidase involves the translocation of cytosolic components (e.g. p47<sup>phox</sup>, p40<sup>phox</sup>, p67<sup>phox</sup>, and p21<sup>rac</sup>) onto membrane-bound proteins (e.g. gp91<sup>phox</sup> and gp22<sup>phox</sup>). THP-1 cells show intracellular expression of NADPH oxidase subunit p67<sup>phox</sup> [20]. We therefore examined whether NADPH oxidase is involved in UVA-induced ROS production in THP-1 cells by monitoring the membrane translocation of p67<sup>phox</sup>. After UVA irradiation, the amount of p67<sup>phox</sup> in the membrane fraction increased (Fig. 2A). Next, we examined the effect of the NADPH oxidase inhibitor DPI. As shown in Fig. 2B, DPI inhibited UVA-mediated ROS production. However, DPI inhibits not only NADPH oxidase, but also mitochondrial complex I, xanthine oxidase, and NO synthase. Therefore,

we also tested inhibitors of each enzyme complex. Pre-incubation with an inhibitor of mitochondrial complex I (rotenone), a xanthine oxidase inhibitor (allopurinol) or a broad-spectrum NO synthase inhibitor (L-NAME) did not block ROS formation (Fig. 2C and D). Taken together, these results indicate that NADPH oxidase is required for UVA-induced ROS production.

### 3.3. UVA irradiation induces ATP release

Released ATP can serve as paracrine signaling molecule for intercellular communication, or it can act in an autocrine manner to regulate cellular functions. We measured the extracellular concentration of ATP in culture medium by means of luciferin-luciferase reaction-based assay. As shown in Fig. 3A, the extracellular concentration of ATP was increased soon after irradiation, and was maintained even at 30 min of post treatment. To identify the pathway of the ATP release, we examined the effects of several inhibitors. ATP release was significantly suppressed by GdCl<sub>3</sub> and arachidonic acid (maxi-anion channel blockers), as well as CBX and probenecid (gap junction hemichannel blockers), while glibenclamide (anion transporter inhibitor) and baflomycin A1 (inhibitor of vesicular H<sup>+</sup>-ATPase) did not block the ATP release (Fig. 3B). These results suggested that release of ATP after UVA irradiation is regulated by plural mechanisms, including maxi-anion channels and hemichannels. We confirmed

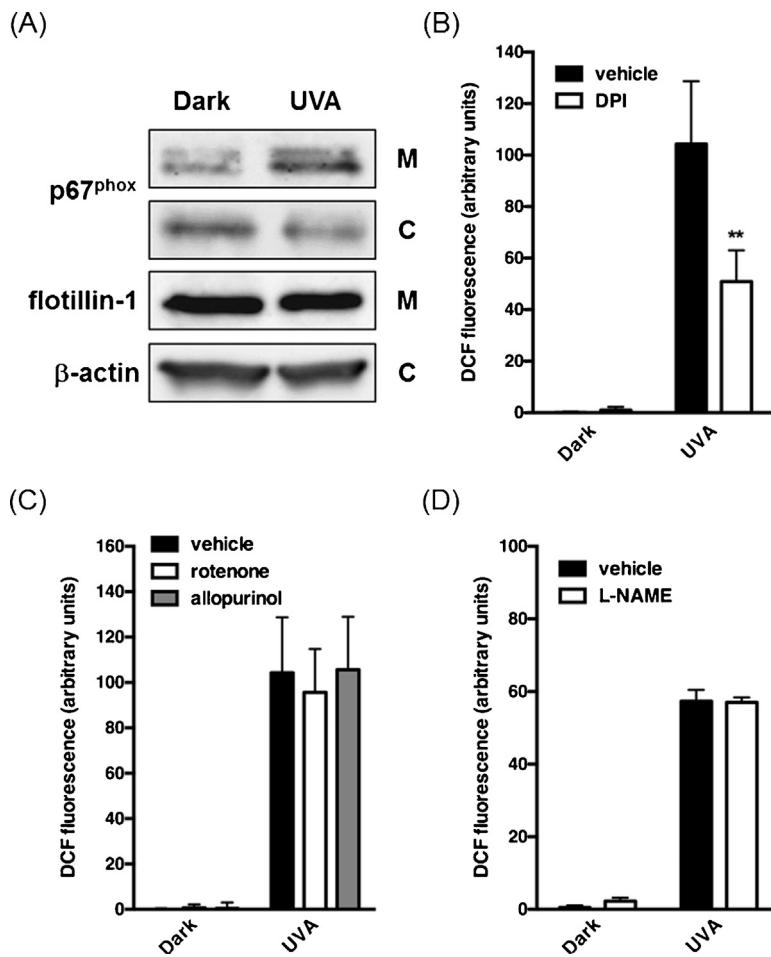


**Fig. 2.** UVA irradiation induces assembly of NADPH oxidase. (A) UVA-irradiated cells were incubated for 5 min. Lysates were fractionated, and the p67<sup>phox</sup> distribution in cytosolic and membrane fractions was analyzed by Western blotting. (B–D) Cells loaded with carboxy-H<sub>2</sub>DCFDA were pre-incubated with (B) DPI (100 μM, 1.5 h) or (C) rotenone (5 μM, 30 min) or allopurinol (100 μM, 30 min); or (D) L-NAME (1 mM, 1 h), then irradiated with 5 J/cm<sup>2</sup>, and incubated for 5 min. The fluorescence was analyzed with a fluorometer. Each value represents the mean ± SD ( $n = 4$ ). Significant differences between the irradiated control groups and the indicated groups are indicated by \*\* ( $P < 0.01$ ).

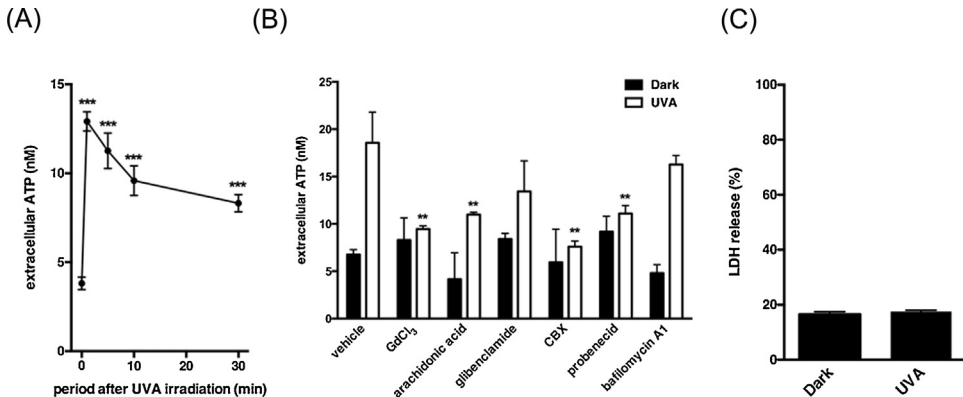


**Fig. 3.** UVA irradiation induces endogenous ATP release. (A) Cells were irradiated with 5 J/cm<sup>2</sup> and incubated for the indicated times. (B) Cells were pretreated with GdCl<sub>3</sub> (50 μM), arachidonic acid (20 μM), glibenclamide (100 μM), CBX (30 μM), probenecid (500 μM) or bafilomycin A (50 nM) for 30 min, then irradiated with 5 J/cm<sup>2</sup>, and 1 min later, the supernatant was collected. In each experiment, the concentration of ATP in the culture medium was measured as described in Section 2. Each value represents the mean ± SD ( $n = 4–8$ ). Significant differences between the time point 0 or irradiated control groups and the indicated groups are indicated by \*\* ( $P < 0.01$ ) and \*\*\* ( $P < 0.001$ ), respectively. (C) Cells were irradiated with 5 J/cm<sup>2</sup> and incubated for 30 min. At the end of incubation, the supernatant was collected and the LDH content was measured. Release of LDH is expressed as a percentage of the total content determined by lysing an equal number of cells with lysis buffer. Each value represents the mean ± SD ( $n = 6$ ).

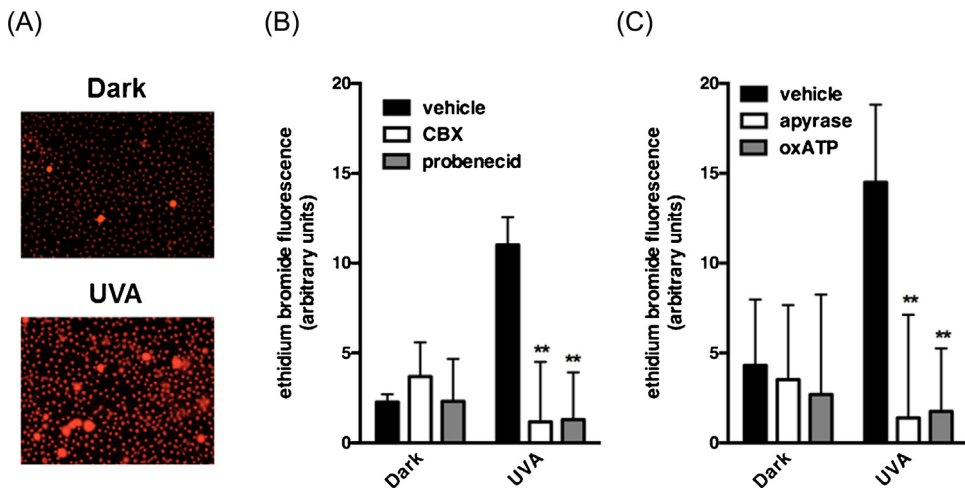


**Fig. 4.** UVA irradiation activates P2X7 receptor. (A) Cells were irradiated with  $5\text{ J/cm}^2$  UVA, and then EtBr ( $25\text{ }\mu\text{M}$ ) was added to the culture medium for 5 min. The change in fluorescence intensity of EtBr was determined by fluorescence microscopy. (B) Cells were pre-incubated with CBX ( $30\text{ }\mu\text{M}$ ) or probenecid ( $500\text{ }\mu\text{M}$ ) for 30 min, and irradiated with  $5\text{ J/cm}^2$  UVA. (C) Cells were pre-incubated with apyrase ( $10\text{ U/mL}$ ) or oxATP ( $300\text{ }\mu\text{M}$ ) for 30 min, and irradiated with  $5\text{ J/cm}^2$  UVA. In both experiments, cells were incubated with EtBr ( $25\text{ }\mu\text{M}$ ) for 5 min after irradiation, and the fluorescence was measured with a fluorometer. Each value represents the mean  $\pm$  SD ( $n=4$ ). Significant differences between the irradiated control groups and the indicated groups are indicated by \*\* ( $P<0.01$ ).

that UVA irradiation did not induce cell death within 30 min (Fig. 3C), suggesting that leakage of ATP from dead cells is not a major route of UVA-induced ATP release.

#### 3.4. UVA-induced ROS production is mediated by P2X7 receptor activation

Extracellular ATP binding to P2X7 ion channels has been proposed as a mechanism of ROS production. It has been reported that activation of P2X7 receptor induces ROS generation through Nox2-based NADPH oxidase in monocytes/macrophages [15]. Since ATP is released from cells after UVA irradiation, P2X7 receptor might be activated. It is known that P2X7 receptor is coupled to hemichannels, leading to the opening of a large plasma membrane pore, which is permeable to large-molecular-mass dyes [21]. To investigate whether P2X7 receptor is activated upon exposure to UVA, we evaluated pore formation by measuring the influx of EtBr. As shown in Fig. 4A, UVA irradiation induced uptake of EtBr into the cells. The fluorescence intensity increased in UVA-irradiated cells, but pretreatment with CBX or probenecid significantly reduced the increase in fluorescence triggered by UVA (Fig. 4B). Uptake of EtBr was also decreased by pretreatment with ectonucleotidase, apyrase, and a pharmacological antagonist of P2X7 receptor, oxATP (Fig. 4C). These results suggested that UVA irradiation leads to activation of P2X7 receptor.

We next evaluated the role of P2X7 receptor in ROS production. Translocation of the cytosolic factor p67<sup>phox</sup> to the plasma membrane by UVA stimulation was prevented by apyrase or oxATP pretreatment (Fig. 5A). In addition, treatment with apyrase or oxATP blocked the stimulatory effect of UVA on ROS production (Fig. 5B). To confirm the involvement of P2X7 receptor in UVA-irradiation-induced ROS production, we silenced the expression

of P2X7 receptor with siRNA. In cells transfected with P2X7-siRNA, P2X7 receptor protein expression was impaired (Fig. 5C). UVA-induced ROS production was also decreased in cells transfected with siRNA for P2X7 receptor (Fig. 5D). Taken together, our results indicate that ATP released into extracellular space activated P2X7 receptor, which in turn activated NADPH oxidase, resulting in ROS production.

#### 3.5. Apoptosis triggered by UVA irradiation is partially mediated by P2X7 receptor activation

To investigate whether the caspase pathway is involved in UVA-induced cell damage, cell viability was analyzed using Z-VAD-FMK (a broad-spectrum caspase inhibitor). Exposure to UVA resulted in a significant decrease in cell viability, but inhibition of the caspase pathway markedly reduced the decrease of cell viability (Fig. 6A). Next, we examined UVA-induced expression of apoptosis markers such as cleaved caspase-9 and -3 by Western blotting. As shown in Fig. 6B, UVA irradiation significantly enhanced caspase activation at the 3 h time point.

To investigate whether UVA-induced apoptosis was mediated through ROS and/or P2X7 receptor, THP-1 cells were pretreated with L-aa or oxATP. Pretreatment with L-aa or oxATP partially blocked the UVA-induced decrease of cell viability, as well as the expression of cleaved caspase-9 and -3 (Fig. 7A and B). Furthermore, the morphological characteristics of apoptotic cells were investigated by staining with Hoechst 33342. Exposure to UVA significantly increased condensation of chromatin. This condensation was blocked by pretreatment with L-aa or oxATP (Fig. 7C). UVA-induced caspase activation and apoptotic nuclei were also suppressed in P2X7-knockdown cells (Fig. 8A and B). These results show that P2X7-mediated ROS production triggered by UVA contributes at least in part to apoptosis.

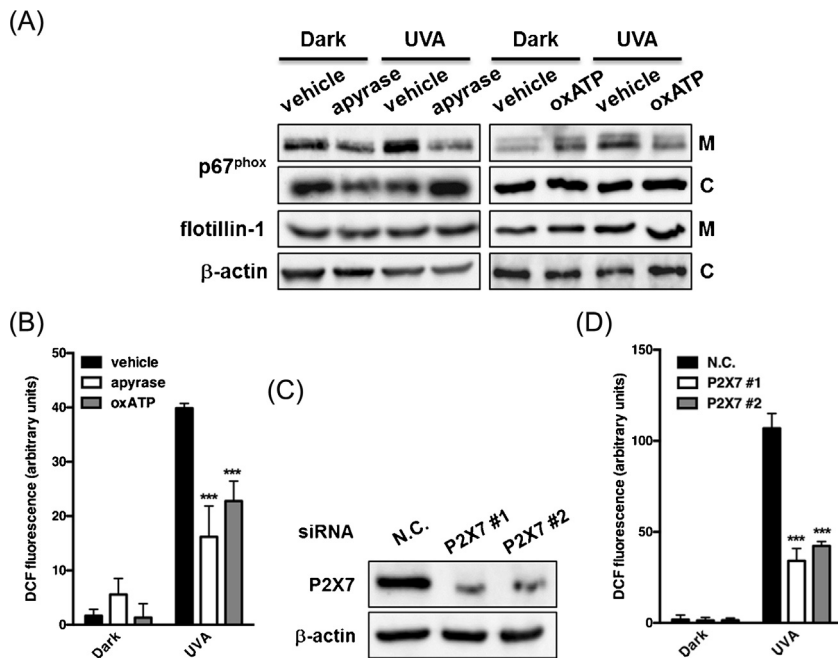


**Fig. 5.** P2X7 receptor is required for UVA-induced ROS production. (A) Cells were pre-incubated with apyrase (10 U/mL) or oxATP (300 μM) for 30 min, then irradiated with 5 J/cm<sup>2</sup> UVA, and incubated for 5 min. Lysates were fractionated, and the p67<sup>phox</sup> distribution in cytosolic and membrane fractions was analyzed by Western blotting. (B) The same experiment was run using cells loaded with carboxy-H<sub>2</sub>DCFDA. The fluorescence was analyzed with a fluorometer; each value represents the mean ± SD ( $n=4$ ). (C) Cells were transfected with siRNA for negative control or P2X7 receptor and incubated for 48 h. Protein expression of P2X7 receptor was determined by Western blotting. (D) siRNA-transfected cells loaded with carboxy-H<sub>2</sub>DCFDA were irradiated with 5 J/cm<sup>2</sup> UVA. The fluorescence was measured with a fluorometer; each value represents the mean ± SD ( $n=4$ ). Significant differences between the irradiated control groups and the indicated groups are indicated by \*\*\* ( $P<0.001$ ).

#### 4. Discussion

Little is known about the effect of UVA irradiation on monocytes. Here, we found that UVA irradiation induces ATP release from THP-1 cells, and this ATP induces ROS generation through activation of P2X7 receptor and NADPH oxidase. Previous studies have suggested that the release

of ATP from THP-1 cells in response to stimuli activates P2X7 receptor and regulates inflammatory responses in an autocrine or a paracrine manner [17,22]. Our present findings are the first evidence that UVA exposure leads to autocrine ATP signaling in THP-1 cells.

Excessive UVA irradiation can cause immunosuppression and photocarcinogenesis, and ROS play a key role

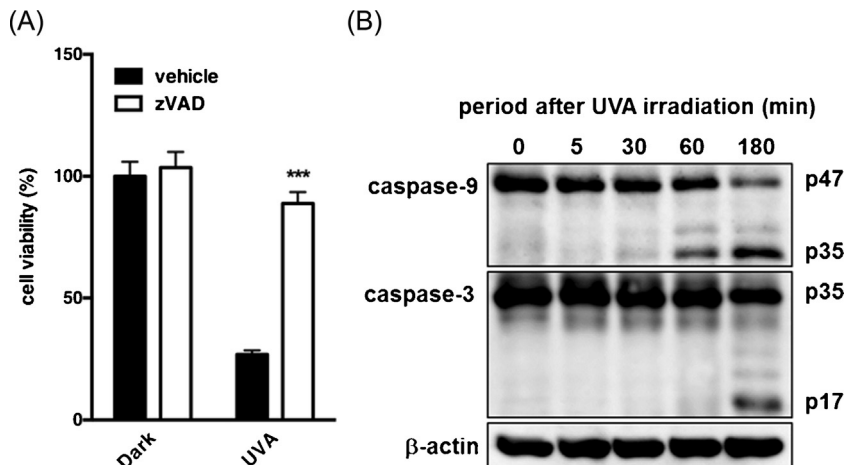


**Fig. 6.** UVA irradiation decreases cell viability by inducing apoptosis. (A) Cells were pre-incubated with z-VAD-FMK (25 μM) for 30 min, then irradiated with 5 J/cm<sup>2</sup> UVA, and incubated for 3 h. After the incubation, cell viability was determined by MTT assay as described in Section 2. Each value represents the mean ± SD ( $n=6$ ). Significant differences between the irradiated control groups and the indicated groups are indicated by \*\*\* ( $P<0.001$ ). (B) After irradiation with 5 J/cm<sup>2</sup> UVA, cells were incubated for the indicated times. At the end of incubation, cell lysates were prepared and expression of caspase-9 and -3 was evaluated by Western blotting.

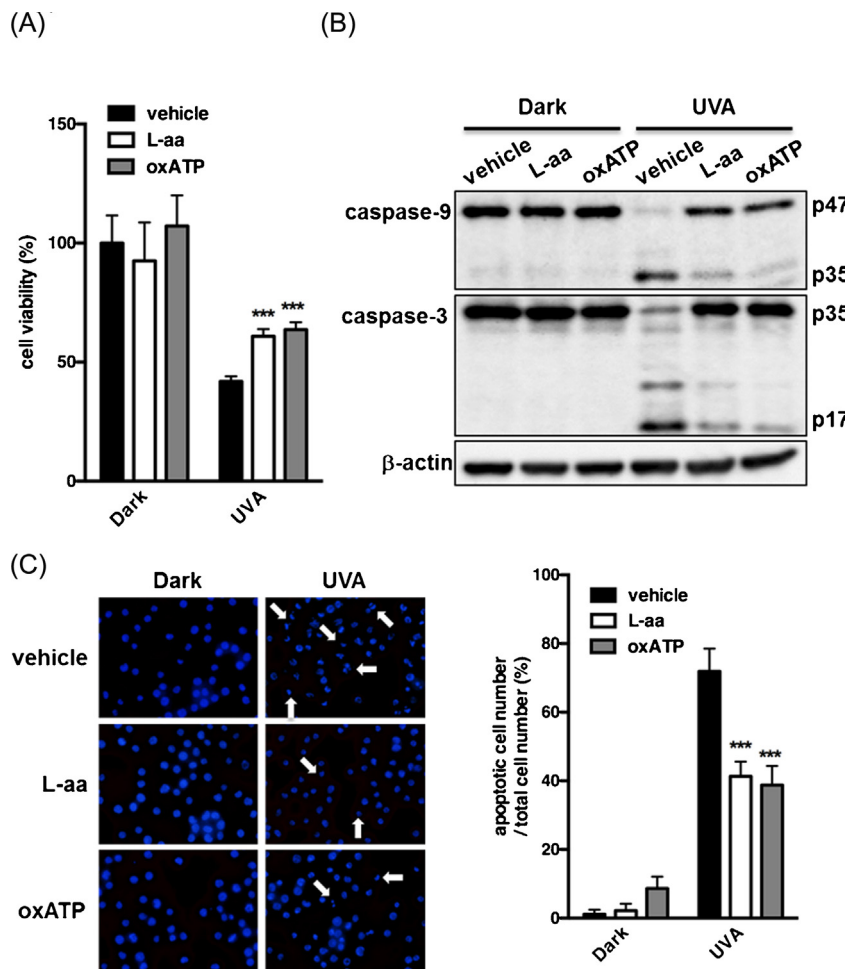


**Fig. 7.** Involvement of ROS and P2X7 receptor in UVA-induced apoptosis. Cells were pre-incubated with L-aa (1 mM) or oxATP (300  $\mu$ M) for 30 min, then irradiated with 5 J/cm<sup>2</sup> UVA, and incubated for 3 h. (A) Cell viability was determined by MTT assay as described in Section 2. Each value represents the mean  $\pm$  SD ( $n = 6$ ). (B) Cell lysates were prepared and expression of caspase-9 and -3 was measured by Western blotting. (C) Nuclear fragmentation was assessed by fluorescence microscopy using Hoechst 33342 (1  $\mu$ g/mL). The number of apoptotic cells in each field was counted; each value represents the mean  $\pm$  SD ( $n = 4\text{--}8$ ). Significant differences between the irradiated control groups and the indicated groups are indicated by \*\*\* ( $P < 0.001$ ).

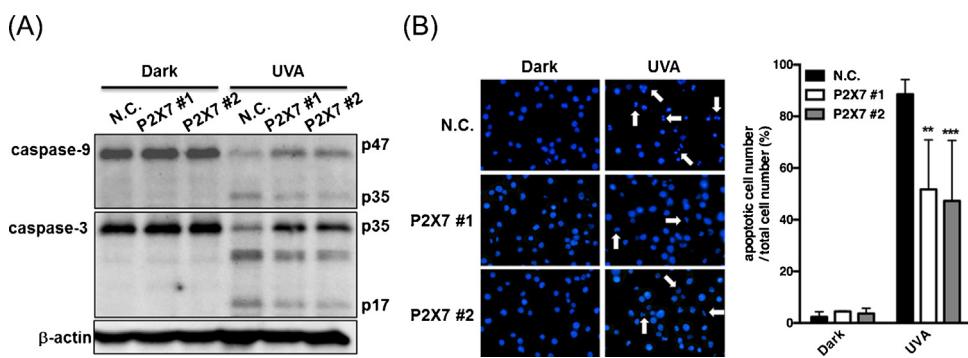


**Fig. 8.** Effect of P2X7 receptor knockdown on UVA-induced apoptosis. Cells were transfected with siRNA for negative control or P2X7 receptor and incubated for 48 h. siRNA-transfected cells were irradiated with 5 J/cm<sup>2</sup> UVA, and incubated for 3 h. (A) Cell lysates were prepared and expression of caspase-9 and -3 was measured by Western blotting. (B) Nuclear fragmentation was assessed by fluorescence microscopy using Hoechst 33342 (1  $\mu$ g/mL). The number of apoptotic cells in each field was counted; each value represents the mean  $\pm$  SD ( $n = 3\text{--}7$ ). Significant differences between the irradiated control groups and the indicated groups are indicated by \*\* ( $P \leq 0.01$ ) and \*\*\* ( $P \leq 0.001$ ).

in this process. Among ROS,  $^1\text{O}_2$  is generally believed to be the first species formed from triplet excited states of endogenous photosensitizers. However,  $^1\text{O}_2$  has a very short lifetime in cells [8,9], so that other ROS, such as  $\text{O}_2^-$ , play key roles [11,23]. We first investigated whether UVA irradiation leads to ROS production using carboxy-H<sub>2</sub>DCFDA, which is not sensitive to  $^1\text{O}_2$  [24]. We found that THP-1 cells showed immediate and sustained production of ROS following UVA irradiation.

NADPH oxidase produces ROS in response to various stimuli, through a complex series of protein/protein interactions [25]. We demonstrated that UVA irradiation resulted in translocation of p67<sup>phox</sup> to the plasma membrane. It is conceivable that UVA-stimulated THP-1 cells produced  $\text{O}_2^-$  via NADPH oxidase activation, since UVA-induced ROS were sensitive to inhibition of NADPH oxidase by DPI and ROS formation was blocked by pretreatment with a SOD mimetic. Released  $\text{O}_2^-$  is converted into hydrogen peroxide by superoxide dismutase, and hydrogen peroxide can diffuse into the same cell, or nearby cells, to elicit responses. Our results indicate that the first phase of ROS production after UVA treatment is NADPH oxidase in THP-1 cells.

Under normal conditions, ATP and other nucleotides are present intracellularly. However, when tissues are injured, stretched, or under stress, cells release large amounts of ATP and other nucleotides in a controlled manner and the released nucleotides serve as local autocrine or paracrine signaling molecules that regulate cell functions [26]. Our results showed that THP-1 cells released ATP just after UVA irradiation. ATP can activate P2X7 receptor and stimulate a variety of responses, including formation of a non-specific pore permeable to small molecules (<900 Da), activation of mitogen-activated protein kinases (MAPKs), activation of NADPH oxidase complex, and formation of ROS [27]. Measurement of EtBr uptake has been previously used to assess P2X7 receptor-mediated pore formation activity. UVA irradiation induces EtBr uptake, indicating that P2X7 receptor is activated by UVA irradiation. We therefore suspected that ATP release and subsequent activation of P2X7 receptor might contribute to ROS production. In accordance with this idea, elimination of extracellular ATP with apyrase or treatment with P2X7 receptor antagonist oxATP effectively reduced both the translocation of p67<sup>phox</sup> and ROS production induced by UVA. Blockade of autocrine signaling mediated by release of ATP and activation of P2X7 receptor in UVA-induced ROS production could therefore be a target for relief of oxidative stress in monocytes.

ATP release mechanisms are highly variable and depend upon cell type and/or stimulus. We excluded the possibility that the increase of extracellular ATP level caused by UVA is related to cell lysis, since UVA irradiation did not induce LDH release into the culture medium within 30 min. On the other hand, Cx43-based hemichannels and the volume-regulated anion channel (VRAC) have been implicated as ATP release pathways [28–30]. Recent evidence also suggests that exocytosis participates in ATP release from activated THP-1 cells [31]. Our findings indicated that at least maxi-anion channel and hemichannels are involved in the release of ATP from UVA-irradiated cells,

although the mechanisms were not fully worked out. Since P2X7 receptor requires high concentration of extracellular ATP ( $\geq 100 \mu\text{M}$ ) for activation, the ATP concentration measured in monocyte culture fluids appears to be well below the threshold required to stimulate P2X7 receptor. However, ecto-nucleotidases, which convert ATP to ADP, AMP, and adenosine, are expressed in monocytes [32], and it is very likely that the measured extracellular ATP levels significantly underestimate the amount of ATP actually released at the cell surface, because of the fast diffusion and rapid hydrolysis of cell-derived ATP [33]. Thus, the concentration of ATP at the cell surface might be sufficient to activate P2X7 receptor.

Several studies have demonstrated that uncontrolled release of ROS plays a role in UVA-induced cell death in various cell lines [23,34]. Cell death is an important component of the innate immune systems, leading to either resolution or propagation of inflammation. Apoptosis generally results in the clearance of host cells by phagocytic cells before release of their inflammatory contents, but if there are large numbers of apoptotic cells, damaged cells may not be completely removed, resulting in induction of inflammation. Our study showed that UVA-induced P2X7 receptor activation triggers  $\text{O}_2^-$  production, which may lead to caspase-dependent apoptosis. However, it is conceivable that other mechanisms are also involved in apoptosis, since antioxidant or P2X7 receptor antagonist did not fully block UVA-induced apoptosis. Apoptosis can be mediated by the cell-surface death receptor and/or by mitochondrial pathways. The former usually involves the Fas and TNF mechanisms followed by activation of caspase-8 [35]. The mitochondrial pathway involves the release of cytochrome c and activation of caspase-9 [36]. Previous reports showed that  $^1\text{O}_2$  initiates Fas receptor clustering and FADD association with aggregated Fas, and triggers apoptosis associated with caspase-8-mediated cytochrome c release and caspase-3 activation [37,38]. In addition, caspase-8-mediated rapid apoptosis has been observed in UVA-treated cells [39]. P2X7 receptor might participate in UVA-induced caspase-dependent cell death independently of the  $^1\text{O}_2$ -mediated apoptotic pathway. Further studies are required to elucidate UVA-induced apoptotic pathways.

## 5. Conclusion

In the present study we have uncovered a novel mechanism of UVA-induced ROS production in THP-1 cells, by demonstrating that UVA irradiation stimulates NADPH oxidase activation through ATP release and subsequent activation of P2X7 receptor. Dendritic cells (DCs) are also distributed in dermis. Since P2X7 receptor also involves inflammatory events in DCs [40], the same phenomenon might be observed. We think it would be worthwhile to investigate further the role of ATP-P2X7 receptor signaling in UVA-mediated cellular responses in a wide range of skin cells, such as primary monocytes and DCs. Our findings suggest that a precise understanding of purinergic signaling might help us to develop new strategies for ameliorating UVA-induced oxidative damage.

## Transparency document

The Transparency document associated with this article can be found in the online version.

## Acknowledgement

This work was supported in part by a Kitasato University Research Grant for Young Researchers.

## References

- [1] C. Marionnet, C. Pierrard, F. Lejeune, J. Sok, M. Thomas, F. Bernerd, Different oxidative stress response in keratinocytes and fibroblasts of reconstructed skin exposed to non extreme daily-ultraviolet radiation, *PLoS ONE* 5 (2010) e12059.
- [2] N.A. Soter, Acute effects of ultraviolet radiation on the skin, *Semin. Dermatol.* 9 (1990) 11–15.
- [3] M.C. Polderman, C. van Kooten, N.P. Smit, S.W. Kamerling, S. Pavel, Ultraviolet-A (UVA-1) radiation suppresses immunoglobulin production of activated B lymphocytes in vitro, *Clin. Exp. Immunol.* 145 (2006) 528–534.
- [4] M. Ichihashi, M. Ueda, A. Budiyanto, T. Bito, M. Oka, M. Fukunaga, K. Tsuru, T. Horikawa, UV-induced skin damage, *Toxicology* 189 (2003) 21–39.
- [5] D.R. Bickers, M. Athar, Oxidative stress in the pathogenesis of skin disease, *J. Invest. Dermatol.* 126 (2006) 2565–2575.
- [6] G.T. Wondrak, M.K. Jacobson, E.L. Jacobson, Endogenous UVA-photosensitizers: mediators of skin photodamage and novel targets for skin photoprotection, *Photochem. Photobiol. Sci.* 5 (2006) 215–237.
- [7] K. Ito, S. Kawanishi, Site-specific DNA damage induced by UVA radiation in the presence of endogenous photosensitizer, *Biol. Chem.* 378 (1997) 1307–1312.
- [8] E. Skovsen, J.W. Snyder, J.D. Lambert, P.R. Ogilby, Lifetime and diffusion of singlet oxygen in a cell, *J. Phys. Chem. B* 109 (2005) 8570–8573.
- [9] R.W. Redmond, I.E. Kochevar, Spatially resolved cellular responses to singlet oxygen, *Photochem. Photobiol.* 82 (2006) 1178–1186.
- [10] A. Valencia, I.E. Kochevar, Nox1-based NADPH oxidase is the major source of UVA-induced reactive oxygen species in human keratinocytes, *J. Invest. Dermatol.* 128 (2008) 214–222.
- [11] A.B. Petersen, R. Gnadecki, J. Vicanova, T. Thorn, H.C. Wulf, Hydrogen peroxide is responsible for UVA-induced DNA damage measured by alkaline comet assay in HaCaT keratinocytes, *J. Photochem. Photobiol. B* 59 (2000) 123–131.
- [12] G. Collo, S. Neidhart, E. Kawashima, M. Kosco-Vilbois, R.A. North, G. Buell, Tissue distribution of the P2X7 receptor, *Neuropharmacology* 36 (1997) 1277–1283.
- [13] A. Surprenant, F. Rassendren, E. Kawashima, R.A. North, G. Buell, The cytolytic P2Z receptor for extracellular ATP identified as a P2X receptor (P2X7), *Science* 272 (1996) 735–738.
- [14] C. Virginio, A. MacKenzie, R.A. North, A. Surprenant, Kinetics of cell lysis, dye uptake and permeability changes in cells expressing the rat P2X7 receptor, *J. Physiol.* 519 (Pt 2) (1999) 335–346.
- [15] T. Noguchi, K. Ishii, H. Fukutomi, I. Naguro, A. Matsuzawa, K. Takeda, H. Ichijo, Requirement of reactive oxygen species-dependent activation of ASK1-p38 MAPK pathway for extracellular ATP-induced apoptosis in macrophage, *J. Biol. Chem.* 283 (2008) 7657–7665.
- [16] M. Tsukimoto, M. Maehata, H. Harada, A. Ikari, K. Takagi, M. Degawa, P2X7 receptor-dependent cell death is modulated during murine T cell maturation and mediated by dual signaling pathways, *J. Immunol.* 177 (2006) 2842–2850.
- [17] A. Piccini, S. Carta, S. Tassi, D. Lasiglie, G. Fossati, A. Rubartelli, ATP is released by monocytes stimulated with pathogen-sensing receptor ligands and induces IL-1beta and IL-18 secretion in an autocrine way, *Proc. Natl. Acad. Sci. U. S. A.* 105 (2008) 8067–8072.
- [18] M.S. Matsui, N. Wang, D. MacFarlane, V.A. DeLeo, Long-wave ultraviolet radiation induces protein kinase C in normal human keratinocytes, *Photochem. Photobiol.* 59 (1994) 53–57.
- [19] H. Hernandez-Pigeon, C. Jean, A. Charruyer, M.J. Haure, C. Baudouin, M. Charveron, A. Quillet-Mary, G. Laurent, UVA induces granzyme B in human keratinocytes through MIF: implication in extracellular matrix remodeling, *J. Biol. Chem.* 282 (2007) 8157–8164.
- [20] Y.L. Siow, K.K. Au-Yeung, C.W. Woo, O. Karmin, Homocysteine stimulates phosphorylation of NADPH oxidase p47<sup>phox</sup> and p67<sup>phox</sup> subunits in monocytes via protein kinase C $\beta$  activation, *Biochem. J.* 398 (2006) 73–82.
- [21] P. Pelegrin, A. Surprenant, Pannexin-1 mediates large pore formation and interleukin-1beta release by the ATP-gated P2X7 receptor, *EMBO J.* 25 (2006) 5071–5082.
- [22] Y.H. Liao, Y.C. Lin, S.T. Tsao, Y.C. Lin, A.J. Yang, C.T. Huang, K.C. Huang, W.W. Lin, HMG-CoA reductase inhibitors activate caspase-1 in human monocytes depending on ATP release and P2X7 activation, *J. Leukoc. Biol.* 93 (2013) 289–299.
- [23] B.R. Zhou, H.B. Yin, Y. Xu, D. Wu, Z.H. Zhang, Z.Q. Yin, F. Permatasari, D. Luo, Baicalin protects human skin fibroblasts from ultraviolet A radiation-induced oxidative damage and apoptosis, *Free Radic. Res.* 46 (2012) 1458–1471.
- [24] P. Bilski, A.G. Belanger, C.F. Chignell, Photosensitized oxidation of 2',7'-dichlorofluorescein: singlet oxygen does not contribute to the formation of fluorescent oxidation product 2',7'-dichlorofluorescein, *Free Radic. Biol. Med.* 33 (2002) 938–946.
- [25] K. Bedard, K.H. Krause, The NOX family of ROS-generating NADPH oxidases: physiology and pathophysiology, *Physiol. Rev.* 87 (2007) 245–313.
- [26] R.S. Ostrom, C. Gregorian, P.A. Insel, Cellular release of and response to ATP as key determinants of the set-point of signal transduction pathways, *J. Biol. Chem.* 275 (2000) 11735–11739.
- [27] Y.I. Lenertz, M.L. Gavala, L.M. Hill, P.J. Bertics, Cell signaling via the P2X(7) nucleotide receptor: linkage to ROS production, gene transcription, and receptor trafficking, *Purinergic Signal* 5 (2009) 175–187.
- [28] K. Hisadome, T. Koyama, C. Kimura, G. Droogmans, Y. Ito, M. Oike, Volume-regulated anion channels serve as an auto/paracrine nucleotide release pathway in aortic endothelial cells, *J. Gen. Physiol.* 119 (2002) 511–520.
- [29] V. Parpura, E. Scemes, D.C. Spray, Mechanisms of glutamate release from astrocytes: gap junction hemichannels, purinergic receptors and exocytotic release, *Neurochem. Int.* 45 (2004) 259–264.
- [30] F. Anselmi, V.H. Hernandez, G. Crispino, A. Seydel, S. Ortolano, S.D. Roper, N. Kessaris, W. Richardson, G. Rickheit, M.A. Filippov, H. Monyer, F. Mammano, ATP release through connexin hemichannels and gap junction transfer of second messengers propagate Ca<sup>2+</sup> signals across the inner ear, *Proc. Natl. Acad. Sci. U. S. A.* 105 (2008) 18770–18775.
- [31] H. Sakaki, M. Tsukimoto, H. Harada, Y. Moriyama, S. Kojima, Autocrine regulation of macrophage activation via exocytosis of ATP and activation of P2Y11 receptor, *PLoS ONE* 8 (2013) e59778.
- [32] S.B. Coade, J.D. Pearson, Metabolism of adenine nucleotides in human blood, *Circ. Res.* 65 (1989) 531–537.
- [33] J. Karczewska, L. Martyniec, G. Dzierzko, J. Stepinski, S. Angielski, The relationship between constitutive ATP release and its extracellular metabolism in isolated rat kidney glomeruli, *J. Physiol. Pharmacol.* 58 (2007) 321–333.
- [34] S. Narayananpillai, C. Agarwal, C. Tilley, R. Agarwal, Silibinin is a potent sensitizer of UVA radiation-induced oxidative stress and apoptosis in human keratinocyte HaCaT cells, *Photochem. Photobiol.* 88 (2012) 1135–1140.
- [35] A. Ashkenazi, V.M. Dixit, Death receptors: signaling and modulation, *Science* 281 (1998) 1305–1308.
- [36] A. Takahashi, Caspase: executioner and undertaker of apoptosis, *Int. J. Hematol.* 70 (1999) 226–232.
- [37] S. Zhuang, M.C. Lynch, I.E. Kochevar, Caspase-8 mediates caspase-3 activation and cytochrome c release during singlet oxygen-induced apoptosis of HL-60 cells, *Exp. Cell Res.* 250 (1999) 203–212.
- [38] S. Zhuang, J.T. Demirs, I.E. Kochevar, Protein kinase C inhibits singlet oxygen-induced apoptosis by decreasing caspase-8 activation, *Oncogene* 20 (2001) 6764–6776.
- [39] S. Zhuang, I.E. Kochevar, Ultraviolet A radiation induces rapid apoptosis of human leukemia cells by Fas ligand-independent activation of the Fas death pathways, *Photochem. Photobiol.* 78 (2003) 61–67.
- [40] F.C. Weber, P.R. Esser, T. Muller, J. Ganesan, P. Pellegatti, M.M. Simon, R. Zeiser, M. Idzko, T. Jakob, S.F. Martin, Lack of the purinergic receptor P2X(7) results in resistance to contact hypersensitivity, *J. Exp. Med.* 207 (2010) 2609–2619.
- [41] M.S. Matsui, V.A. DeLeo, Longwave ultraviolet radiation and promotion of skin cancer, *Cancer Cells* 3 (1991) 8–12.
- [42] D.P. Steenvoorden, G.M. van Henegouwen, The use of endogenous antioxidants to improve photoprotection, *J. Photochem. Photobiol. B* 41 (1997) 1–10.
- [43] D.E. Godar, UVA1 radiation triggers two different final apoptotic pathways, *J. Invest. Dermatol.* 112 (1999) 3–12.